



## UWS Academic Portal

### E3 and M2 transition strengths in Bi-209(83)

Roberts, O. J.; Ni, C.R.; Bruce, A. M.; Mrginean, N.; Bucurescu, D.; Deleanu, D.; Filipescu, D.; Florea, N. M.; Gheorghe, I.; Ghi, D.; Glodariu, T.; Lica, R.; Mrginean, R.; Mihai, C.; Negret, A.; Sava, T.; Stroe, L.; uvil, R.; Toma, S.; Alharbi, T.; Alexander, T.; Aydin, S.; Brown, B. A.; Browne, F.; Carroll, R. J.; Mulholland, K.; Podolyák, Zs.; Regan, P. H.; Smith, J. F.; Smolen, M.; Townsley, C. M.

*Published in:*  
Physical Review C

*DOI:*  
[10.1103/PhysRevC.93.014309](https://doi.org/10.1103/PhysRevC.93.014309)

Published: 14/01/2016

*Document Version*  
Publisher's PDF, also known as Version of record

[Link to publication on the UWS Academic Portal](#)

#### *Citation for published version (APA):*

Roberts, O. J., Ni, C. R., Bruce, A. M., Mrginean, N., Bucurescu, D., Deleanu, D., ... Townsley, C. M. (2016). E3 and M2 transition strengths in Bi-209(83). *Physical Review C*, 93, [014309].  
<https://doi.org/10.1103/PhysRevC.93.014309>

#### **General rights**

Copyright and moral rights for the publications made accessible in the UWS Academic Portal are retained by the authors and/or other copyright owners and it is a condition of accessing publications that users recognise and abide by the legal requirements associated with these rights.

#### **Take down policy**

If you believe that this document breaches copyright please contact [pure@uws.ac.uk](mailto:pure@uws.ac.uk) providing details, and we will remove access to the work immediately and investigate your claim.

**E3 and M2 transition strengths in  $^{209}\text{Bi}$** 

O. J. Roberts,<sup>1,2,\*</sup> C. R. Niță,<sup>1,3</sup> A. M. Bruce,<sup>1</sup> N. Mărginean,<sup>3</sup> D. Bucurescu,<sup>3</sup> D. Deleanu,<sup>3</sup> D. Filipescu,<sup>3</sup> N. M. Florea,<sup>3,4</sup> I. Gheorghe,<sup>3,5</sup> D. Ghiță,<sup>3</sup> T. Glodariu,<sup>3</sup> R. Lica,<sup>3</sup> R. Mărginean,<sup>3</sup> C. Mihai,<sup>3</sup> A. Negret,<sup>3</sup> T. Sava,<sup>3</sup> L. Stroe,<sup>3</sup> R. Șuvăilă,<sup>3</sup> S. Toma,<sup>3</sup> T. Alharbi,<sup>6,7</sup> T. Alexander,<sup>6</sup> S. Aydin,<sup>8</sup> B. A. Brown,<sup>9</sup> F. Browne,<sup>1</sup> R. J. Carroll,<sup>6</sup> K. Mulholland,<sup>10</sup> Zs. Podolyák,<sup>6</sup> P. H. Regan,<sup>6,11</sup> J. F. Smith,<sup>10</sup> M. Smolen,<sup>10</sup> and C. M. Townsley<sup>6</sup>

<sup>1</sup>*School of Computing, Engineering and Mathematics, University of Brighton, Brighton BN2 4GJ, United Kingdom*

<sup>2</sup>*School of Physics, University College Dublin, Belfield, Dublin 4, Ireland*

<sup>3</sup>*Horia Hulubei National Institute of Physics and Nuclear Engineering, P.O. Box MG-6, Bucharest-Magurele, Romania*

<sup>4</sup>*University Politehnica of Bucharest, 011061, Bucharest, Romania*

<sup>5</sup>*Faculty of Physics, University of Bucharest, RO-077125, Bucharest, Romania*

<sup>6</sup>*Department of Physics, University of Surrey, Guildford GU2 7XH, United Kingdom*

<sup>7</sup>*Department of Physics, Almajmaah University, P.O. Box 66, 11952, Saudi Arabia*

<sup>8</sup>*Department of Physics, University of Aksaray, Aksaray, Turkey*

<sup>9</sup>*Department of Physics and Astronomy, and National Superconducting Cyclotron Laboratory, Michigan State University, East Lansing, Michigan 48824-1321, USA*

<sup>10</sup>*Nuclear Physics Research Group, The University of the West of Scotland, Paisley PA1 2BE, United Kingdom*

<sup>11</sup>*National Physics Laboratory, Teddington TW11 0LW, United Kingdom*

(Received 15 June 2015; revised manuscript received 16 November 2015; published 14 January 2016)

The  $1i_{13/2} \rightarrow 1h_{9/2}$  ( $M2$ ) and  $3s_{1/2} \rightarrow 2f_{7/2}$  ( $E3$ ) reduced proton transition probabilities in  $^{209}\text{Bi}$  have been determined from the direct half-life measurements of the  $13/2_1^+$  and  $1/2_1^+$  states using the Romanian array for  $\gamma$ -ray Spectroscopy in HEavy ion REactions (RoSPHERE). The  $13/2_1^+$  and  $1/2_1^+$  states were found to have  $T_{1/2} = 0.120(15)$  ns and  $T_{1/2} = 9.02(24)$  ns respectively. Angular distribution measurements were used to determine an  $E3/M2$  mixing ratio of  $\delta = -0.184(13)$  for the 1609 keV  $\gamma$ -ray transition deexciting the  $13/2_1^+$  state. This value for  $\delta$  was combined with the measured half-life to give reduced transition probabilities of  $B(E3, 13/2_1^+ \rightarrow 9/2_1^-) = 12(2) \times 10^3 e^2 \text{fm}^6$  and  $B(M2, 13/2_1^+ \rightarrow 9/2_1^-) = 38(5)\mu_N^2 \text{fm}^2$ . These values are in good agreement with calculations within the finite Fermi system. The extracted value of  $B(E3, 1/2_1^+ \rightarrow 7/2_1^-) = 6.3(2) \times 10^3 e^2 \text{fm}^6$  can be explained by a small ( $\sim 6\%$ ) admixture in the wave function of the  $1/2_1^+$  state.

DOI: 10.1103/PhysRevC.93.014309

**I. INTRODUCTION**

The ground state of  $^{209}\text{Bi}$  can be described as a single  $1h_{9/2}$  proton coupled to the  $^{208}\text{Pb}$  core [1]. A septuplet of levels with spins between  $3/2$  and  $15/2$ , formed due to the coupling of the same proton to the  $3^-$  octupole vibrational state in the  $^{208}\text{Pb}$  core, is observed at an excitation energy of  $\sim 2.6$  MeV. The three states below this septuplet are predominately formed from the excitation of the single proton [1]. Present information on the properties of low-lying states in  $^{209}\text{Bi}$  was determined from comprehensive inelastic scattering [2–6], Coulomb excitation [7–11], direct decay time [12–14], and multinucleon transfer reaction [1,15] measurements.

In cases where the properties of low-lying excitations in single-nucleon systems are simple to interpret and can be described using basic theoretical models, effective multipole operators have been shown to describe static electric and magnetic multipole moments and low-energy-transition rates [16]. Renormalization effects are incorporated in the effective multipole operators, which, in the case of electric multipoles, mainly arise from the core polarization mechanism [17]. Because the uncertainties for configuration mixing in the lead

region are smaller than in other regions around closed-shell nuclei (e.g.,  $^{16}\text{O}$ ,  $^{40}\text{Ca}$ ), Mottelson has advocated that the lead region is possibly the best place to explore the effective charge phenomena [18]. Therefore, this article presents new measurements on low-lying levels in  $^{209}\text{Bi}$  from which the strength of the single-particle  $1i_{13/2} \rightarrow 1h_{9/2}$  and  $3s_{1/2} \rightarrow 2f_{7/2}$  transitions have been extracted.

The strength of the  $1i_{13/2} \rightarrow 1h_{9/2}$   $M2$  transition can be obtained from the half-life of the  $13/2_1^+$  level and the  $E3/M2$  mixing ratio of the depopulating transition. The latter is required because the  $13/2_1^+$  state ( $E_x = 1609$  keV) is known to be a mixture of a single proton in the  $1i_{13/2}$  shell coupled to the  $0^+$  ground state in the  $^{208}\text{Pb}$  core, and a single proton in the  $1h_{9/2}$  shell coupled to the  $3^-$  octupole vibrational state in  $^{208}\text{Pb}$  [7,19,20], as shown schematically in Fig. 1.

The  $B(E3)$  excitation probability to the  $13/2_1^+$  level has been measured in Coulomb excitation experiments using  $\alpha$  and  $^{16}\text{O}$  beams to be  $12.4(32) \times 10^3 e^2 \text{fm}^6$  [7] and  $22(8) \times 10^3 e^2 \text{fm}^6$  [8] respectively. It has also been independently measured to be  $27(3) \times 10^3 e^2 \text{fm}^6$  [4] and  $20(4) \times 10^3 e^2 \text{fm}^6$  [6] from inelastic scattering of  $^{209}\text{Bi}$ . The last three values are in broad agreement, but the first [7] is considerably smaller. A study by Kratschmer *et al.* [22] suggested that the absolute transition rates deduced from Ref. [7] may not be valid, as the

\*oliver.roberts@ucd.ie

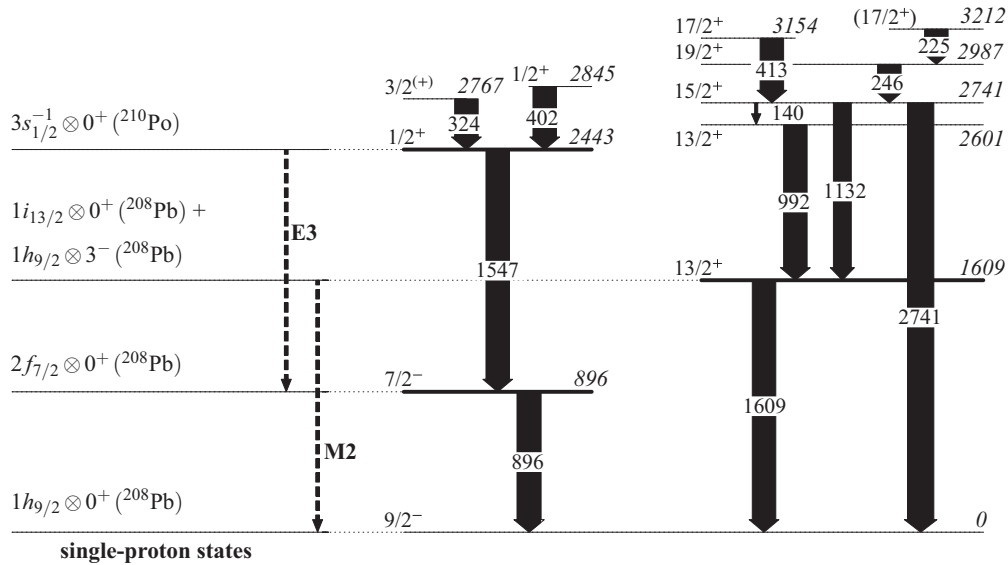


FIG. 1. The partial level scheme of the low-lying states in  $^{209}\text{Bi}$ . The dashed lines represent the pure multipole transitions, for which strengths are extracted in this work. The transition energies are given in keV and the width of the arrows represents the intensity of the transitions normalized to 100% for the strongest transition from each level [21]. The thicker lines denote the levels for which decay spectra were analyzed in this work.

bombarding energy of the  $\alpha$  beam was too high to produce pure Coulomb excitation. However, since the value measured agrees with the value from Hertel *et al.* [8] to within one standard deviation, and the value from Ungrin *et al.* [6] to within two standard deviations, it has been included in the subsequent analysis of this paper.

The  $E3$  admixture in the wave function of the 1609-keV transition depopulating this level has been determined previously to be  $\sim 10\%$  based on a measured mixing ratio of  $-0.33(10)$  [20]. Beene *et al.*, combined this measured mixing ratio with a value of  $B(E3; 1609 \rightarrow 0) = 15(1) \times 10^3 e^2 \text{fm}^6$ , quoted by Bohr and Mottelson [23], to derive a calculated value of  $T_{1/2} = 0.29(15)$  ns [20] for the 1609-keV level. Following the method described by Bohr and Mottelson [23], a weighted average of the results in Refs. [4,6–8], after each has been individually normalised so that the measured  $E3$  excitation probability for the  $1h_{9/2}(3^-)$  septuplet agrees with the assumed value of  $7 \times 10^5 e^2 \text{fm}^6$  for the  $3^-$  vibrational state in  $^{208}\text{Pb}$  [24], gives a  $B(E3; 1609 \rightarrow 0) = 17(3) \times 10^3 e^2 \text{fm}^6$ . Combining this value of the  $B(E3 \downarrow)$  with a measured mixing ratio of  $-0.33(10)$  [20] for the 1609-keV transition yields  $T_{1/2} = 0.26(14)$  ns. Prior to this current work, there has not been a direct measurement of the half-life.

The strength of the  $3s_{1/2} \rightarrow 2f_{7/2}$  pure  $E3$  transition can be obtained from the half-life of the first  $\frac{1}{2}^+$  state at 2443 keV. This has been previously measured to be  $T_{1/2} = 11.3(4)$  ns [3] and  $T_{1/2} = 10(2)$  ns [25]. The  $\frac{19}{2}^+$  level at 2987 keV is known to be isomeric with a half-life of 17.9(5) ns [3], but its lifetime could not be measured in this work.

## II. EXPERIMENTAL SET-UP

Excited states in  $^{209}\text{Bi}$  were populated by bombarding an enriched ( $\sim 99\%$ ),  $20 \text{ mg cm}^{-2}$   $^{208}\text{Pb}$  target with a 32-MeV

$^7\text{Li}$  beam, delivered by the 9 MV tandem accelerator at the National Institute for Physics and Nuclear Engineering in Bucharest, Romania. The  $^{208}\text{Pb}(^7\text{Li}, 2n\alpha\gamma)^{209}\text{Bi}$ , proton transfer reaction at around the barrier energy, was estimated to be  $\sim 4\%$  of the total reaction cross section [26]. Nuclei that were also produced in this experiment include  $^{210}\text{Bi}$  [27,28],  $^{212}\text{Po}$  [29], and  $^{212,213}\text{At}$  [29,30], with the strongest side channel being attributed to the  $3n$  fusion-evaporation reaction ( $^{212}\text{At}$ ).

The half-lives of the levels of interest were measured using  $\gamma$  rays detected in RoSPHERE, which is an array of 14 Compton-suppressed high-purity germanium (HPGe) detectors and 11  $\text{LaBr}_3(\text{Ce})$  scintillator detectors. The  $\text{LaBr}_3(\text{Ce})$  and HPGe detectors were all placed  $\sim 20$  cm from the target position at forward and backward angles of  $37^\circ$ ,  $70^\circ$ , and  $90^\circ$  relative to the beam axis. The 11 cylindrical  $\text{LaBr}_3(\text{Ce})$  detectors in this setup comprised seven  $2''$  diameter by  $2''$  long crystals, and four  $1.5''$  diameter by  $2''$  long crystals. All 11 detectors were doped with 5% of  $\text{Ce}^{3+}$ . The data were recorded using either a HPGe-HPGe-HPGe or a HPGe- $\text{LaBr}_3(\text{Ce})$ - $\text{LaBr}_3(\text{Ce})$  triggering condition with a coincidence master gate time window of  $\sim 50$  ns. A total of  $\sim 3.5 \times 10^7$  HPGe- $\text{LaBr}_3(\text{Ce})$ - $\text{LaBr}_3(\text{Ce})$  coincidences were recorded during the five-day experiment. The energy and efficiency calibrations for both the HPGe and  $\text{LaBr}_3(\text{Ce})$  detectors were obtained using  $^{152}\text{Eu}$  and  $^{60}\text{Co}$  sources. The timing response of each detector was corrected offline for the low-energy time walk using a  $^{152}\text{Eu}$  source, as described in Ref. [31].

For the angular distribution measurement, the  $20 \text{ mg cm}^{-2}$   $^{208}\text{Pb}$  target was orientated at  $55^\circ$  relative to the beam axis. A coaxial detector, at a distance of 30 cm from the target position, was used to measure  $\gamma$ -ray intensities at 16 angles between  $-26.5^\circ$  and  $+116.5^\circ$ . A clover detector placed at  $90^\circ$  relative to the beam axis acted as the monitor detector. Efficiencies at each of the measured angles were performed using both  $^{60}\text{Co}$

and  $^{152}\text{Eu}$  sources, placed at the target position. Lead shielding was placed in front of both the moving and monitor detectors in an effort to reduce contamination lines from tantalum, which was present in both the beam stopper and collimator. Discs of copper, cadmium, and aluminum were also placed around the front of both the moving and monitor HPGe detectors in order to reduce the detection of x rays. The current of the  $^7\text{Li}$  beam on the  $^{208}\text{Pb}$  target was roughly  $\sim 8$  p nA during the measurement at each angle.

### III. DATA ANALYSIS AND RESULTS

The half-life data was collected and sorted offline into a series of  $\gamma$ -ray energy and time difference spectra, two-dimensional HPGe and  $\text{LaBr}_3(\text{Ce})$  ( $E_\gamma$ - $E_\gamma$ ) matrices, and three-dimensional  $E_{\gamma_1}$ - $E_{\gamma_2}$ - $\Delta T$  cubes, and subsequently analysed using the GASPWARE and RADWARE packages [32,33]. Figure 2(a) shows a projection of the HPGe  $E_\gamma$ - $E_\gamma$  matrix, where the transitions used as gates in the HPGe detectors to select the cascades required in the  $\text{LaBr}_3(\text{Ce})$  detectors to

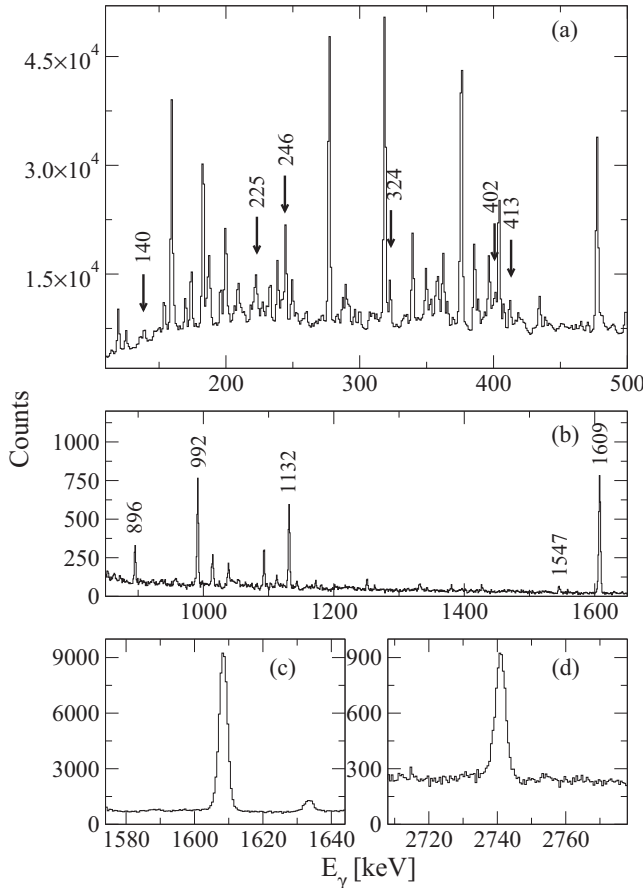


FIG. 2. The  $\gamma$ -ray energy spectra measured in the HPGe detectors: (a) The total projection of an  $E_\gamma$ - $E_\gamma$  matrix, with the 140-, 225-, 246-, 324-, 402-, and 413-keV  $^{209}\text{Bi}$  transitions used as gates marked by arrows. (b) An energy spectrum created as a result of using the gates in panel (a), with the high-energy  $\gamma$ -ray transitions of interest in  $^{209}\text{Bi}$  labeled with their energy. Panels (c) and (d) show the cleanliness of the 1609- and 2741-keV transitions in the singles spectra, used for the angular distribution analysis.

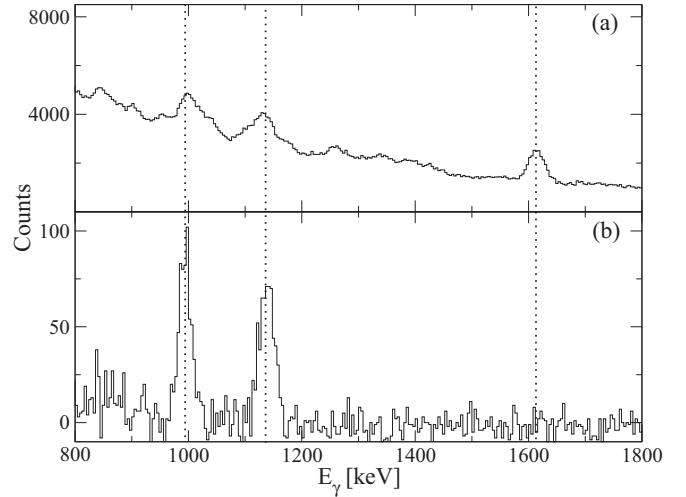


FIG. 3. The  $\gamma$ -ray energy spectra measured in the  $\text{LaBr}_3(\text{Ce})$  detectors: (a) The total projection of the  $E_\gamma$ - $E_\gamma$  matrix with gates in the HPGe detectors on the 140-, 225-, 246-, and 413-keV transitions, and (b) with the addition of a gate on the 1609-keV transition in a  $\text{LaBr}_3(\text{Ce})$  detector. The dashed lines indicate the positions of the feeding (992- and 1132-keV) and deexciting (1609-keV) transitions for the  $\frac{13}{2}^+$  state.

measure the  $\frac{13}{2}^+$  and  $\frac{7}{2}^-$  levels are denoted by the arrows. The cleanliness of this procedure can be seen in Fig. 2(b), where the transitions that were used to obtain the decay spectra are indicated. The corresponding  $\text{LaBr}_3(\text{Ce})$  spectra are shown in Fig. 3, where (a) shows the result of applying gates on the 140-, 225-, 246-, and 413-keV transitions in the HPGe detectors, and (b) the result of applying an additional gate on the 1609 keV transition in a  $\text{LaBr}_3(\text{Ce})$  detector. The spectrum in Fig. 3(b) shows that it is possible to set clean gates in the  $\text{LaBr}_3(\text{Ce})$  detectors on the 992- and 1132-keV transitions which feed the 1609-keV state.

Figure 4(a) shows the forward and reverse time-difference spectra for the 896 keV level, obtained by gating on the photopeaks of the feeding and deexciting 1547- and 896-keV  $\gamma$ -ray transitions on the energy axes of an  $E_{\gamma_1}$ - $E_{\gamma_2}$ - $\Delta T$  cube [31]. The cube was sorted with gates on the 324- and 402-keV transitions in the HPGe detectors. The half-life of the  $\frac{7}{2}^-$  level was previously calculated to be  $T_{\frac{1}{2}} = 8.2(12)$  ps based on the weighted average of the  $B(E2 \uparrow)$  values from Refs. [1,8,22] and the adopted mixing ratio from Ref. [34]. This value of the half-life is consistent with the lack of a centroid shift between the two distributions in Fig. 4(a) and was used to determine a timing resolution of  $\sim 350$  ps full width at half maximum (FWHM) for the setup. The centroid shift measurement of the  $\frac{13}{2}^+$  level uses gates on the photopeaks of the  $\frac{13}{2}^+ \rightarrow \frac{13}{2}^+$  (992-keV),  $\frac{15}{2}^+ \rightarrow \frac{13}{2}^+$  (1132-keV) and  $\frac{13}{2}^+ \rightarrow \frac{9}{2}^-$  (1609-keV) transitions shown in Figs. 3(a) and 3(b). The timing distributions of the 992- and 1609-keV and the 1132- and 1609-keV coincidences were summed to give the forward and reverse time-difference spectra shown in Fig. 4(b). The difference between these symmetric time distributions is twice the lifetime and gives a value of  $T_{\frac{1}{2}} = 0.120(15)$  ns

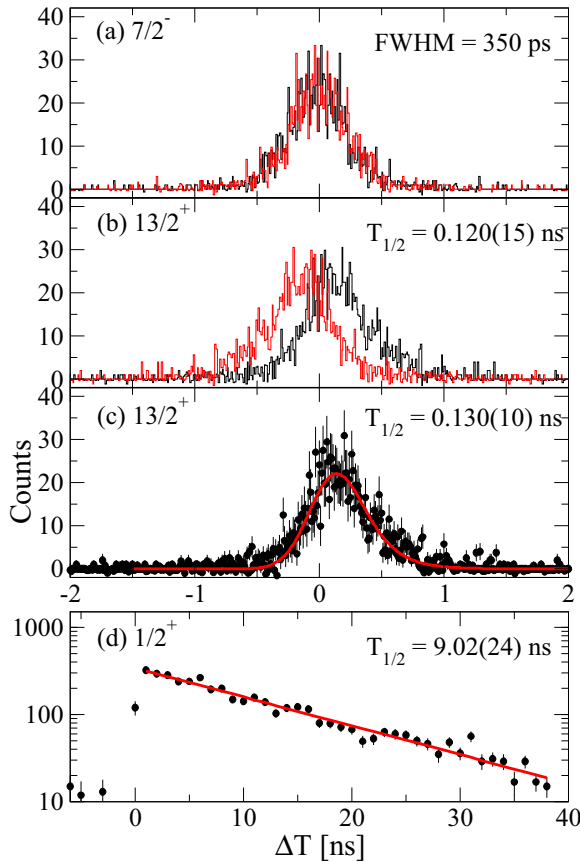


FIG. 4. The forward (black) and reverse (red) time distributions for (a) the 896-keV state, obtained by gating on the 1547- and 896-keV coincidences and (b) the 1609-keV state, obtained by gating on the photopeaks of the feeding (992- and 1132-keV) and deexciting (1609-keV) transitions. The forward time profile of (c) the 1609-keV state uses the same gates as in (b) and (d). The forward time profile of the 2443-keV state was obtained by gating on the photopeaks of the feeding (324- and 402-keV) and deexciting (1547- and 896-keV) transitions.

for the  $\frac{13}{2}^+$  level. Figure 4(c) shows the individual points of the time curve for the same data, including the associated statistical uncertainty. This time curve was fitted with a convolution between the prompt response function (PRF) shown in Fig. 4(a) and an exponential decay function. This method gives a value of  $T_{\frac{1}{2}} = 0.130(10)$  ns, which is in good agreement with the value from the centroid shift method. However, this value has an uncertainty of only 10 ps, which is equivalent to the time resolution of the setup and is therefore thought to be underestimated. The accepted value of the half-life to be used in the subsequent discussions is therefore  $T_{\frac{1}{2}} = 0.120(15)$  ns.

The forward time distribution of the  $\frac{1}{2}^+$  isomeric state in Fig. 4(d), was obtained by gating on the 896- and 1547-keV transitions in the HPGe detectors and on the photopeaks of the feeding (324- and 402-keV) and deexciting (1547- and 896-keV)  $\gamma$ -ray transitions in the LaBr<sub>3</sub>(Ce) detectors. Figure 1 shows that applying these gates in the HPGe detectors will produce very clean energy spectra in the LaBr<sub>3</sub>(Ce)

detectors due to the lack of any side-feeding into the cascade of interest. The resulting time distribution, shown in Fig. 4(d) with 1 ns binning, yields a value of  $T_{\frac{1}{2}} = 9.02(24)$  ns. This value is significantly greater than the prompt time resolution of  $\sim 350$  ps [Fig. 4(a)], and is within one standard deviation of the value reported by Ellegaard *et al.* [25], but differs significantly from the value of Demanins and Raichich [3]. Due to the lack of details on the data analysis in Ref. [3], the source of the discrepancy between these values is ambiguous, but may be clarified in future studies.

In order to resolve the  $B(E3)$  and  $B(M2)$  contributions to the  $1i_{\frac{13}{2}} \rightarrow 1h_{\frac{9}{2}}$  transition strength, the angular distribution of the 1609-keV transition was measured. Singles spectra as a function of angle were obtained for the 246-, 1609-, and 2741-keV transitions which depopulate the  $\frac{19}{2}^+$ ,  $\frac{13}{2}^+$ , and  $\frac{15}{2}^+$  levels respectively, as shown in Fig. 1. These transitions were the only transitions in  $^{209}\text{Bi}$  which were sufficiently clean or had enough statistics for an angular distribution measurement. The cleanliness of the 1609- and 2741-keV transitions in the HPGe singles spectrum is shown in Figs. 2(c) and 2(d) respectively. The measured  $\gamma$ -ray intensities as a function of angle, shown in Fig. 5, were interpreted using the expression [35]

$$W(\theta) = A_0(1 + A_2 B_2 P_2(\cos \theta) + A_4 B_4 P_4(\cos \theta) + A_6 B_6 P_6(\cos \theta)), \quad (1)$$

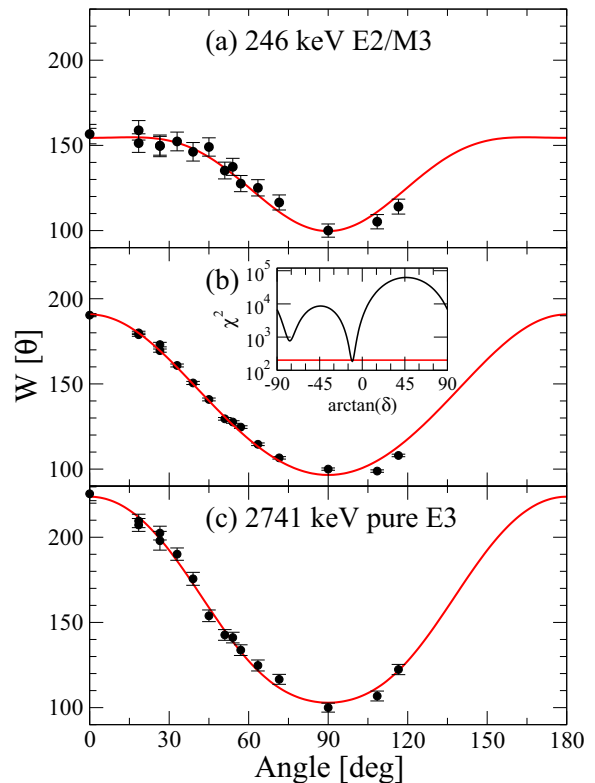


FIG. 5. The  $\gamma$ -ray intensity as a function of angle for the (a) 246 mixed  $E2/M3$  transition, (b) 1609-keV transition, and (c) 2741 keV pure  $E3$  transition. The inset to (b) shows the  $\chi^2$  value as a function of  $\arctan(\delta)$ .

TABLE I. Half-lives and measured and calculated  $B(L\lambda)$  transition rates in  $^{209}\text{Bi}$ .

$E_x$ (keV)	$J_i^\pi$	$T_{1/2}$ (ns)	$E_\gamma$ (keV)	$J_f^\pi$	$L\lambda$	Measured transitions	$B(L\lambda)$ ( $\times 10^3 e^2 \text{fm}^6$ or $\mu_N^2 \text{fm}^2$ )	SM ( $\times 10^3 e^2 \text{fm}^6$ or $\mu_N^2 \text{fm}^2$ )	FFS ( $\times 10^3 e^2 \text{fm}^6$ or $\mu_N^2 \text{fm}^2$ )
1609	$\frac{13}{2}^+$	0.120(15)	1609	$\frac{9}{2}^-$	E3	$(^{208}\text{Pb } 3^- \otimes \pi 1h_{9/2}) \rightarrow (^{208}\text{Pb } 0^+ \otimes \pi 1h_{9/2})$	12(2)	0.52	9.8 [40]
					M2	$(^{208}\text{Pb } 0^+ \otimes \pi 1i_{13/2}) \rightarrow (^{208}\text{Pb } 0^+ \otimes \pi 1h_{9/2})$	0.038(5)	0.43	0.033 [41]
2443	$\frac{1}{2}^+$	9.02(24)	1547	$\frac{7}{2}^-$	E3	$(^{210}\text{Po } 0^+ \otimes \pi 3s_{1/2}) \rightarrow (^{208}\text{Pb } 0^+ \otimes \pi 2f_{7/2})$	6.3(2)	0	

where  $A_0$  is a normalizing factor and the  $A_{2,4,6}$  coefficients depend on the spins of the states involved in the transition and the mixing ratio of the  $\gamma$  ray. The  $B_{2,4,6}$  coefficients contain the alignment of the initial state, which was considered to be a Gaussian distribution centered about  $M = 0$  and parametrized as [36]

$$w(M) = N \exp[(-0.5M/\sigma)^2], \quad (2)$$

where  $N$  is a normalizing factor such that  $\sum w(M) = 1$  and  $\sigma$  is a parameter in the fit.  $P_{2,4,6}(\cos \theta)$  are the standard Legendre polynomial functions. The data were fitted using the STAG code which follows the method outlined in Ref. [36].

The 2741-keV transition decays from the  $\frac{15}{2}^+$  level to the  $\frac{9}{2}^-$  ground state and was used to evaluate the parameter  $\sigma$ , used in the alignment distribution described by Eq. (2) on the assumption that it is a stretched E3 transition. Figure 5(c) shows the best fit to this data which was obtained with a value of  $\sigma = 2.25$ , corresponding to  $\frac{\sigma}{J} = 0.30$ . Using this as a starting point, the best fit for the 246-keV ( $\frac{19}{2}^+ \rightarrow \frac{15}{2}^+$ ) transition [shown in Fig. 5(a)], was obtained for values of  $\sigma = 2.24$  ( $\frac{\sigma}{J} = 0.24$ ) and  $\delta = 0.02(2)$ . The error on  $\delta$  was obtained following the procedure outlined in Ref. [37]. The value of  $\delta = 0.02(2)$  is consistent with the expectation of a small M3 admixture in the  $\Delta J = 2$  transition. The best fit to the data for the 1609-keV transition between the  $\frac{13}{2}^+ \rightarrow \frac{9}{2}^-$  states is shown in Fig. 5(b). The inset to Fig. 5(b) shows the variation of  $\chi^2$  for the fit as a function of the mixing ratio of the transition, with the red line indicating a value of  $\chi^2$  which is 1.09 times the minimum. This is the multiplier calculated [37] for 13 degrees of freedom [16 data points minus 3 parameters ( $A_0, \delta, \sigma$ ) in the fit] and gives the value of  $\chi^2$  used to evaluate the error in delta. The best fit for this level was obtained for values of  $\sigma = 2.14$  ( $\frac{\sigma}{J} = 0.33$ ) and  $\delta = -0.184(13)$ . The value of  $\delta$  which corresponds to  $\sigma = 2.25$  is  $\delta = -0.20$ .

The half-lives of the 1609- and 2443-keV states and the mixing ratio of the 1609-keV transition have been used in the following equations to derive the reduced transition probabilities [38]:

$$B(M2) = \frac{5.12 \times 10^{-8}}{T_{1/2} E_\gamma^5} \frac{1}{(1 + \delta_{\frac{E3}{M2}}^2)} \mu_N^2 \text{fm}^2 \quad (3)$$

and

$$B(E3) = \frac{1.21 \times 10^{-3}}{T_{1/2} E_\gamma^7} \frac{\delta_{\frac{E3}{M2}}^2}{(1 + \delta_{\frac{E3}{M2}}^2)} e^2 \text{fm}^6, \quad (4)$$

where  $E_\gamma$  is the  $\gamma$ -ray energy in MeV and  $T_{1/2}$  is the half-life of the state in seconds. The  $B(L\lambda)$  values obtained using these equations are listed in Table I.

The value quoted in Sec. I for the weighted average of previous measurements of  $B(E3, \frac{13}{2}^+ \rightarrow \frac{9}{2}^-) = 17(3) \times 10^3 e^2 \text{fm}^6$  is within one standard deviation of the value of  $B(E3, \frac{13}{2}^+ \rightarrow \frac{9}{2}^-) = 12(2) \times 10^3 e^2 \text{fm}^6$  that has been determined from the measured half-life and mixing ratio in this work. Excluding the value from Broglia *et al.* [7] from the weighted average gives a value of  $B(E3, \frac{13}{2}^+ \rightarrow \frac{9}{2}^-) = 20(2) \times 10^3 e^2 \text{fm}^6$  from previous work. This is two standard deviations from the  $12(2) \times 10^3 e^2 \text{fm}^6$  extracted from the current measurements, which therefore supports the validity of Broglia's measurement.

#### IV. DISCUSSION

Shell-model calculations in which the lowest  $\frac{13}{2}^+$  and  $\frac{9}{2}^-$  states are described as pure  $\pi 1i_{13/2}$  and  $\pi 1h_{9/2}$  configurations and the radial wave functions are obtained with the Skx Skyrme mean-field approximation [39] yield  $B(E3, \frac{13}{2}^+ \rightarrow \frac{9}{2}^-) = 0.52 \times 10^3 e^2 \text{fm}^6$  and  $B(M2, \frac{13}{2}^+ \rightarrow \frac{9}{2}^-) = 0.43 \times 10^3 \mu_N^2 \text{fm}^2$  with free-nucleon charges and  $g$  factors. These values are at least an order of magnitude different from the experimental values shown in Table I with the calculated  $B(E3)$  value being too small and the calculated  $B(M2)$  being too large. Calculations within the theory of finite Fermi systems (FFS), which takes into account the residual interaction between quasiparticles, eliminating the need for effective charges [40] yield  $B(E3, \frac{13}{2}^+ \rightarrow \frac{9}{2}^-) = 9.8 \times 10^3 e^2 \text{fm}^6$ . This value was calculated by adjusting the parameters of the effective particle-hole interactions. Calculations with an effective magnetic operator give  $B(M2, \frac{13}{2}^+ \rightarrow \frac{9}{2}^-) = 33 \mu_N^2 \text{fm}^2$  [41]. Both of these values are in good agreement with the measured ones.

The  $\frac{1}{2}^+$  state at 2443 keV was observed to have a large spectroscopic factor in the  $^{210}\text{Po}(t, \alpha)$  [42] reaction and is therefore dominated by the excitation of a proton across the  $Z = 82$  shell gap to form a  $[(\pi 1h_{9/2})_{0+}^2 \otimes (\pi 3s_{1/2}^{-1})]$  configuration. The  $B(E3)$  strength from this configuration to the  $\pi 2f_{7/2}$  state at 896 keV is identically zero. Ellegaard *et al.* [25] suggest that the transition proceeds through an admixture of  $[(\pi 2f_{7/2})_{0+}^2 \otimes (\pi 3s_{1/2}^{-1})]$  in the wave function of the  $E_x = 2443$  keV  $\frac{1}{2}^+$  state. Shell-model calculations with an effective proton charge of 1.6 give a  $B(E3) = 7.9 \times 10^3 e^2 \text{fm}^6$  for the  $[(\pi 2f_{7/2})_{0+}^2 \otimes (\pi 3s_{1/2}^{-1})] \rightarrow \pi 2f_{7/2}$  transition. Allowing the admixture of all the 1p-1h

states considered in Ref. [43], gives a  $B(E3,[(\pi 2f_{7/2}^2)_{0^+}^2 \otimes (\pi 3s_{1/2}^{-1})] \rightarrow [\pi 2f_{7/2}^2]) = 95 \times 10^3 e^2 \text{fm}^6$ , due to the admixture of the low-lying  $3^-$  state of  $^{208}\text{Pb}$ . A 6% admixture of this wave function into the pure configuration involving the  $\pi 1h_{9/2}$  is required to explain the experimental value, in agreement with the result obtained by Ellegaard *et al.* [25].

## V. SUMMARY

The results of the measurement of the half-life of the  $\frac{13}{2}^+$  level [ $T_{1/2} = 0.120(15) \text{ns}$ ] and the  $E3/M2$  mixing ratio for the 1609-keV transition [ $\delta = -0.184(13)$ ] have been combined to give  $B(E3, \frac{13}{2}^+ \rightarrow \frac{9}{2}^-) = 12(2) \times 10^3 e^2 \text{fm}^6$  and  $B(M2, \frac{13}{2}^+ \rightarrow \frac{9}{2}^-) = 38(5) \mu_N^2 \text{fm}^2$ . The results of calculations performed within the single-particle shell model are unable to reproduce these values, but better agreement is obtained with calculations within the finite Fermi system [40,41].

The half-life of the long-lived  $\frac{1}{2}^+$  state at 2443 keV was measured to be 9.02(24) ns, which corresponds to

$B(E3, \frac{1}{2}^+ \rightarrow \frac{7}{2}^-) = 6.3(2) \times 10^3 e^2 \text{fm}^6$ . This transition is strictly forbidden in the single-particle shell model but can be explained by a small ( $\sim 6\%$ ) admixture in the wave function of the  $\frac{1}{2}^+$  state [25].

## ACKNOWLEDGMENTS

The staff of the Horia Hulubei National Institute of Physics and Nuclear Engineering (IFIN-HH), Bucharest, Romania are thanked for their excellent technical support during this experiment. This work was supported by a UK NuSTAR grant (ST/G000697/1) from the Science and Technology Facilities Council (STFC) and by NSF Grant No. PHY-1404442. O.J.R. acknowledges support from Science Foundation Ireland under Grant No. 12/IP/1288. T.A. acknowledges support from Almajmaah University, Saudi Arabia. The work of N.M.F. has been funded by the Sectoral Operational Programme Human Resources Development 2007-2013 of the Ministry of European Funds through the Financial Agreement POS-DRU/159/1.5/S/132397. P.H.R. acknowledges support from the UK National Measurement Office (NMO).

- 
- [1] O. Häusser, F. C. Khanna, and D. Ward, *Nucl. Phys. A* **194**, 113 (1972).
- [2] J. F. Ziegler and G. A. Peterson, *Phys. Rev.* **165**, 1337 (1968).
- [3] F. Demanins and F. Raicich, *Nuovo Cimento A* **109**, 5 (1996).
- [4] A. Scott, M. Owais, and F. Petrovich, *Nucl. Phys. A* **226**, 109 (1974).
- [5] W. Benenson, S. M. Austin, P. J. Locard, F. Petrovich, J. R. Borysowicz, and H. McManus, *Phys. Rev. Lett.* **24**, 907 (1970).
- [6] J. Ungrin, R. M. Diamond, P. O. Tjøm, and B. Elbek, *Mat. Fys. Medd. K. Dan. Vidensk. Selsk.* **38**, 8 (1971).
- [7] R. A. Broglia, J. S. Lilley, R. Perazzo, and W. R. Phillips, *Phys. Rev. C* **1**, 1508 (1970).
- [8] J. W. Hertel, D. G. Fleming, J. P. Schiffer, and H. E. Gove, *Phys. Rev. Lett.* **23**, 488 (1969).
- [9] E. Grosse, M. Dost, K. Haberkant, J. W. Hertel, H. V. Klapdor, H. J. Körner, D. Proetel, and P. Von Brentano, *Nucl. Phys. A* **174**, 525 (1971).
- [10] O. Nathan, *Nucl. Phys.* **30**, 332 (1962).
- [11] D. S. Andreev, J. Z. Gangrskij, C. Lemberg, and V. A. Nabinoritschvili, *Izv. Akad. Nauk. SSSR* **29**, 2231 (1965).
- [12] P. Salling, *Phys. Lett.* **17**, 139 (1965).
- [13] H. J. Körner, K. Auerbach, J. Braunsfurth, and E. Gerdau, *Nucl. Phys.* **86**, 395 (1966).
- [14] J. L. Quebert, K. Nakai, R. M. Diamond, and F. S. Stephens, *Nucl. Phys. A* **150**, 68 (1970).
- [15] O. Häusser, A. B. McDonald, T. K. Alexander, A. J. Ferguson, and R. E. Warner, *Phys. Lett. B* **38**, 75 (1972).
- [16] G. Astner, I. Bergström, J. Blomqvist, B. Fant, and K. Wikström, *Nucl. Phys. A* **182**, 219 (1972).
- [17] A. Bohr and B. R. Mottelson, *Nuclear Structure, Vol I: Nuclear Deformations* (World Scientific, Singapore, 1969), Chap. 3.
- [18] B. R. Mottelson, *Nikko Summer School Lectures 1967*, NORDITA Publication No. 288 (Nordic Institute for Theoretical Physics, Stockholm, 1967).
- [19] K. Arita and H. Horie, *Phys. Lett. B* **30**, 14 (1969).
- [20] J. R. Beene, O. Häusser, T. K. Alexander, and A. B. McDonald, *Phys. Rev. C* **17**, 1359 (1978).
- [21] K. H. Maier, T. Nail, R. K. Sheline, W. Stöfl, J. A. Becker, J. B. Carlson, R. G. Lanier, L. G. Mann, G. L. Struble, J. A. Cizewski, and B. H. Erkkila, *Phys. Rev. C* **27**, 1431 (1983).
- [22] W. Kratschmer, H. V. Klapdor, and E. Grosse, *Nucl. Phys. A* **201**, 179 (1973).
- [23] A. Bohr and B. R. Mottelson, *Nuclear Structure, Vol II: Nuclear Deformations* (World Scientific, Singapore, 1998), Chap. 6, p. 565.
- [24] A. Bohr and B. R. Mottelson, *Nuclear Structure, Vol II: Nuclear Deformations* (World Scientific, Singapore, 1998), Chap. 6, p. 561.
- [25] C. Ellegaard, R. Julin, J. Kantele, M. Luontama, and T. Poikolainen, *Nucl. Phys. A* **302**, 125 (1978).
- [26] O. B. Tarasov and D. Bazin, *Nucl. Instrum. Methods Phys. Res., Sect. B* **204**, 174 (2003).
- [27] H. T. Motz, E. T. Journey, E. B. Shera, and R. K. Sheline, *Phys. Rev. Lett.* **26**, 854 (1971).
- [28] R. K. Sheline, R. L. Ponting, A. K. Jain, J. Kvasil, B. du Nianga, and L. Nkwambiaya, *Czech. J. Phys. B* **39**, 22 (1989).
- [29] T. P. Sjoreen, U. Garg, and D. B. Fossan, *Phys. Rev. C* **21**, 1838 (1980).
- [30] S. Bayer, A. P. Byrne, G. D. Dracoulis, A. M. Baxter, T. Kibédi, F. G. Kondev, S. M. Mullins, and T. R. McGoram, *Nucl. Phys. A* **650**, 3 (1999).
- [31] N. Mărginean, D. L. Balabanski, D. Bucurescu, S. Lalkovski, L. Atanasova, G. Căta-Danil, I. Căta-Danil, J. M. Daugas, D. Deleanu, P. Detistov, G. Deyanova, D. Filipescu, G. Georgiev, D. Ghiță, K. A. Gladnishi, R. Lozeva, T. Glodariu, M. Ivașcu, S. Kisyov, C. Mihai, R. Mărginean, A. Negret, S. Pascu, D. Radulov, T. Sava, L. Stroe, G. Suliman, and N. V. Zamfir, *Eur. Phys. J. A* **46**, 329 (2010).

- [32] D. Bazzacco and N. Mărginean (private communication).
- [33] D. Radford, *Nucl. Instrum. Methods Phys. Res., Sect. A* **361**, 297 (1995).
- [34] G. R. Hagee, R. C. Lange, and J. T. McCarthy, *Nucl. Phys.* **84**, 62 (1966).
- [35] H. Frauenfelder and R. M. Steffen, in  *$\alpha$ ,  $\beta$  and  $\gamma$ -ray Spectroscopy*, edited by K. Siegbahn (North Holland, Amsterdam, 1965).
- [36] P. A. Butler and P. J. Nolan, *Nucl. Instrum. Methods* **190**, 283 (1981).
- [37] A. N. James, P. J. Twin, and P. A. Butler, *Nucl. Instrum. Methods* **115**, 105 (1974).
- [38] K. Alder and R. M. Steffen, *The Electromagnetic Interaction in Nuclear Spectroscopy* (North Holland, Amsterdam, 1975), Chap. 2, p. 39.
- [39] B. A. Brown, *Phys. Rev. C* **58**, 220 (1998).
- [40] P. Ring, R. Bauer, and J. Speth, *Nucl. Phys. A* **206**, 97 (1973).
- [41] R. Bauer, J. Speth, V. Klemt, P. Ring, E. Werner, and T. Yamazaki, *Nucl. Phys. A* **209**, 535 (1973).
- [42] P. D. Barnes, E. Romberg, C. Ellegaard, R. F. Casten, O. Hansen, T. J. Mulligan, R. A. Broglia, and R. Liotta, *Nucl. Phys. A* **195**, 146 (1972).
- [43] B. A. Brown, *Phys. Rev. Lett.* **85**, 5300 (2000).